

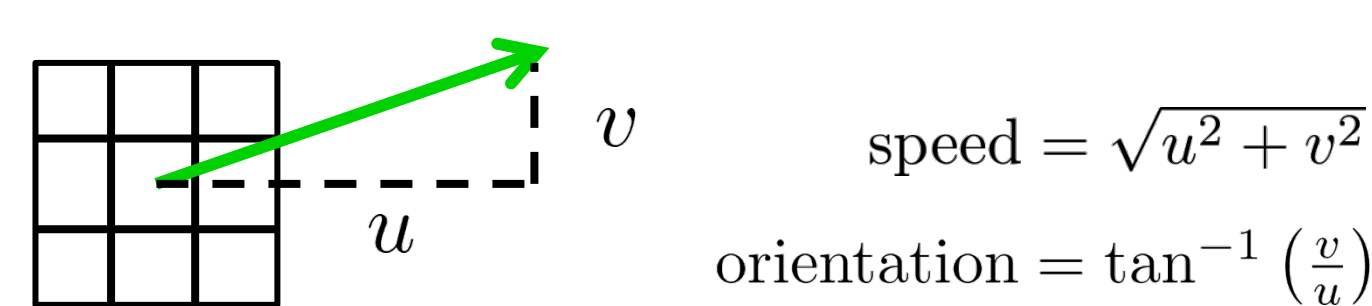
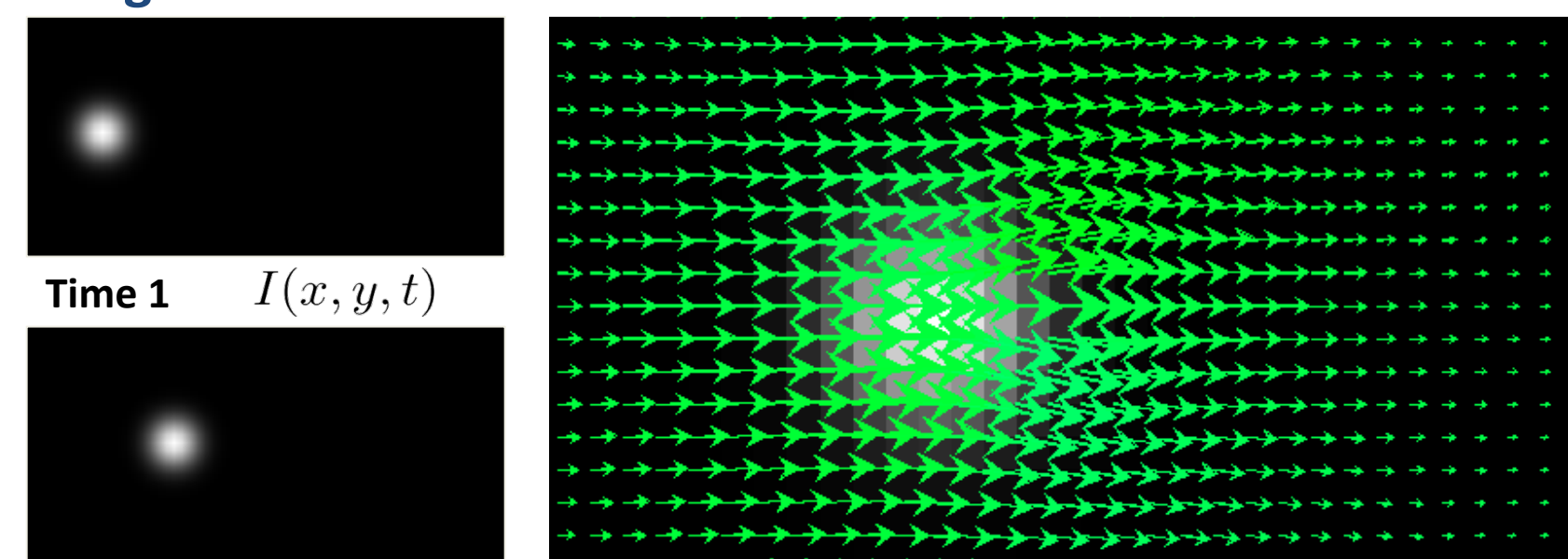
Cell migration, formation of cellular protrusions (e.g. blebs, filopodia), and structural reorganization are important phenomena in cell biology. Precise quantifications of movement/deformation are crucial to understand these processes at different levels of organization. We apply computer vision methods for combined optical flow (OF) and multi-scale (MS) motion estimation of membrane translations, end growing and protrusion formation in fluorescence microscopy images. For these cases we bound OF error and optimal sampling rate, in order to guide biologists on their experimental conditions. We also show the advantages of OF methods compared with manual segmentation and tracking.

Abstract

Introduction

A key question to quantify motion is to determine the movement of each pixel...

A pixel's motion is represented with a vector (u,v) . Over an image this forms a vector field.



If we assume grey value constancy between two successive images at time t and time $t+1$, or

$$I(x, y, t) = I(x + u, y + v, t + 1),$$

the search for the "best" movement of each pixel (u,v) pixel, can be formulated as a minimization problem for $f(u,v)$,

$$f(u, v) = I(x, y, t) - I(x + u, y + v, t + 1) = I_x u + I_y v + I_t.$$

In computer vision, methods to minimize $f(u,v)$ have been proposed assuming different constraints.

Lucas & Kanade LK-OF [1]

Look for (u,v) vectors which are similar in a small image region p , giving more importance to the center,

$$K_p * (I_x u + I_y v + I_t)^2.$$

Horn & Schunck HS-OF [2]

Solutions for (u,v) are required to be also smooth,

$$(I_x u + I_y v + I_t)^2 + \alpha(|\nabla u|^2 + |\nabla v|^2).$$

Bruhn et al. CLG-OF [3]

Solutions for (u,v) are required to give more importance to the local information and also to be smooth,

$$K_p * (I_x u + I_y v + I_t)^2 + \alpha(|\nabla u|^2 + |\nabla v|^2).$$

In order to apply OF methods in biological problems, it is important to know:

- their limits (minimum/maximum speed, error), in order to correctly setup experimental conditions like sampling rate.
- how to estimate optimal method parameters.

We propose how to address both questions in five cases that represent any cell deformation, as shown in the next section.

Materials & Methods

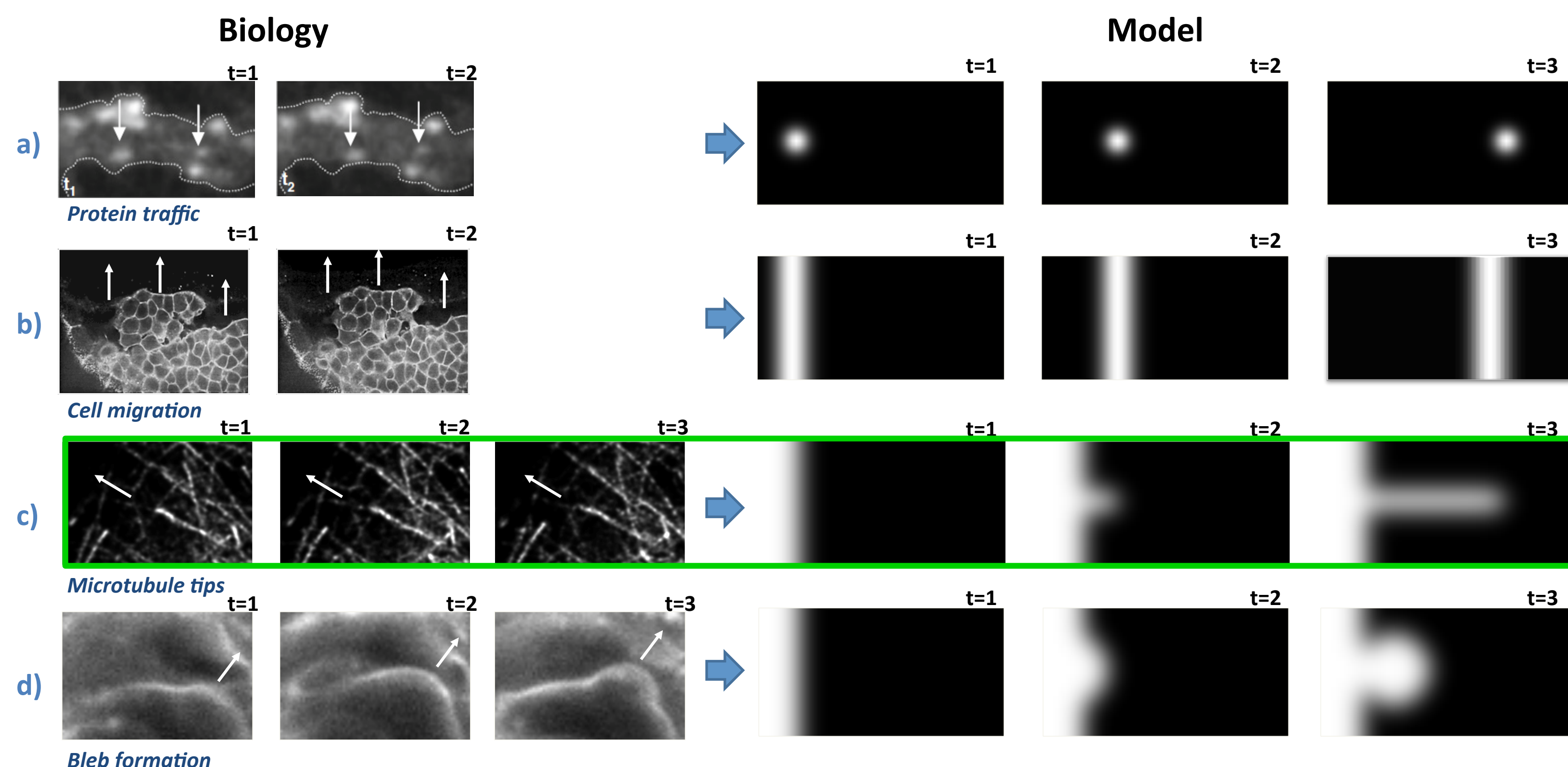


Figure 1. Four dynamical structures and their simplified models.

a) GABA_{R1} receptors traffic in dendrites (first presented by Delpiano et al [4]. b) Cell migration in the Kupffer's vesicle. c) Microtubule reorganization in COS cells. d) Cell bleb formation in the parapineal organ of zebrafish.

Biological systems. COS-7 cells expressing EB3-GFP, pineal cells expressing GFP and dorsal forerunner cells expressing an actine sensor in zebrafish were studied. Live imaging, deconvolution and restoring filters were applied.

Synthetic control sequences. Convolution of microscopic point spread functions with basic morphologic models of single molecules, membranes and protrusions. Different MS-OF approaches combined with active contour models were compared to evaluate vector fields for motion estimation and object segmentation/tracking.

Results

We show that the parameters of the OF methods can be automatically tuned, in order to increase motion range and precision. Next, we compare our OF results with standard methods used by biologists (like tracking) to compute speed, upon manual and automatic segmentation.

I. Theoretical OF parameter optimization

1. For LK-OF, the key step is the inversion of the 2x2 matrix, A . The condition number (κ) quantifies the upper bound error [5].

$$\kappa(A) = \left(\frac{\lambda_{\max}}{\lambda_{\min}}\right)^2 \in (0, 1]; \quad A = \begin{bmatrix} K_p * I_x^2 & K_p * I_x I_y \\ K_p * I_x I_y & K_p * I_y^2 \end{bmatrix}.$$

where λ denotes the eigenvalues of matrix A (function of the edges of the image). Pixels where κ will have bounded confidence. Therefore, selecting those pixels in the area of interest limits the measurement error.

2. For the HS-OF iterative scheme,

$$u_i^{k+1} = \bar{u}_i^k - \frac{I_x(I_x \bar{u}_i^k + I_y \bar{v}_i^k + I_t)}{\alpha^2 + I_x^2 + I_y^2},$$

α^2 is important in areas where $\alpha^2 > I_x^2 + I_y^2$, and thus its value should be equal to the gradient in the areas of interest.

3. For the CLG-OF, a similar argument can be presented:

$$u_i^{k+1} = \frac{\sum_{l=1}^2 \frac{\alpha_l}{h_l^2} \left(\sum_{l \in N_l^-(i)} u_j^{k+1} + \sum_{l \in N_l^+(i)} u_j^{k+1} \right) - (J_{12i} v_i^k + J_{13i} v_i^k)}{\sum_{l=1}^2 \frac{\alpha_l}{h_l^2} |N_l(i)| + J_{11i}},$$

α is important in areas where $\alpha^2 < I_x^2 + I_y^2$, thus its value should be equal to the gradient in the areas of interest.

Note that α from HS-OF is different than CLG-OF, being

$$\alpha_{CLG} = \frac{\alpha_{HS}}{2}$$

II. Numerical evaluation of OF methods and parameter selection for synthetic models

From our model scenarios, we consider the case of tip growing or filopodia (Fig. 1c).

First, we use the error in the speed estimation to find an optimal parameters set when using OF methods (Fig. 2a), and then we test the range of maximum speeds we were able to detect with OF (Fig. 2b).

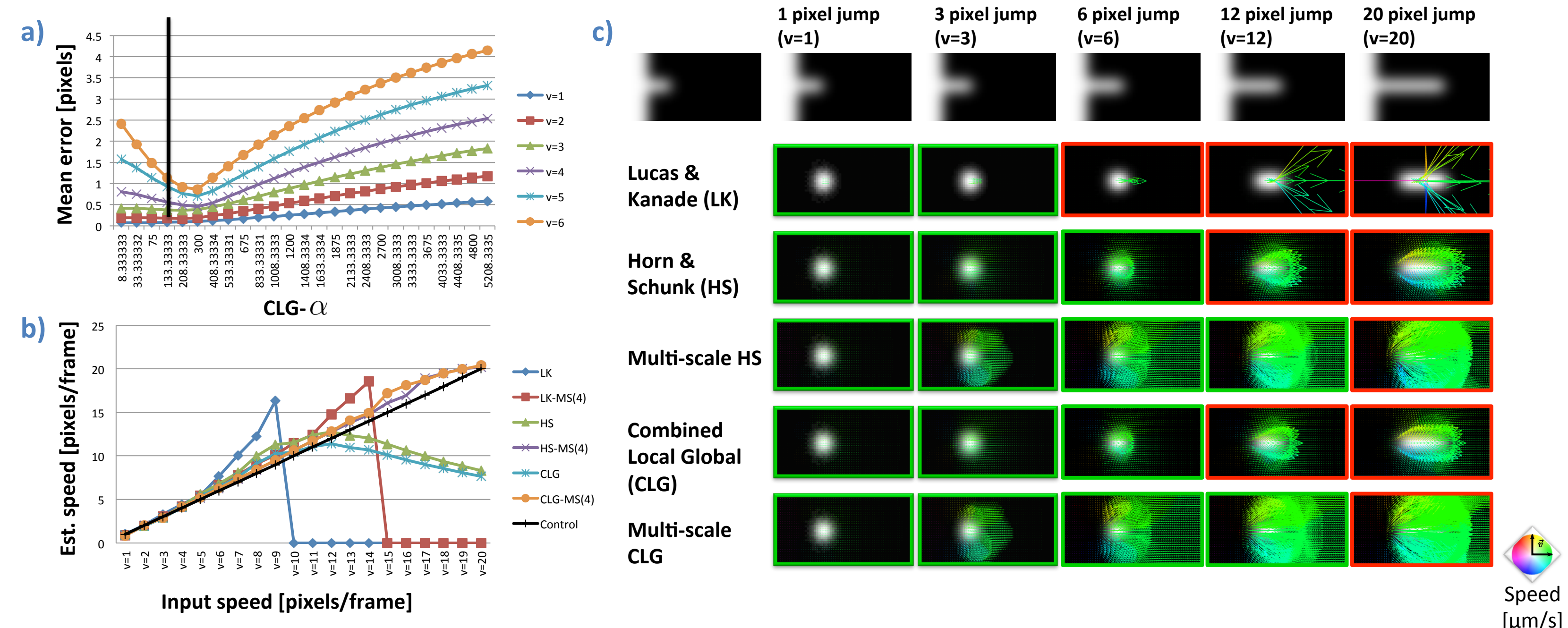


Figure 2. OF methods evaluation for model structures (sample).

- Parameter optimization (α) for CLG-OF method in the tip model (theoretical α shown in black).
- Maximum detectable speeds.
- OF for the tip model at different input speeds, measuring all of the described OF methods.

Multi-scale CLG (MS-CLG) yields the largest range and lowest error: 12 pixels/frame, error < 1. pixel.

For instance, if a pixel corresponds to 0.04 [μ m] (63x objective), an accurate measurement for a movement of 0.08 [μ m/s] requires at least 1 image acquired each 6 seconds.

III. Application to microtubule tip growing (speed detection)

Microtubule network is highly dynamic and it has been shown that it has a typical growing speed due to the underlying molecular mechanism.

Our goal is to verify that the tip speed can be retrieved using OF, and show the advantages of the technique when compared with the standard technique of manually marking and measuring the displacement of each tip.

Microtubule tip segmentation approach:

- First, automatically segment microtubule tip using an intensity threshold on the images.
- Second, manual refinement leaving only the tips that appear in three consecutive frames.

We compare different speed estimation approaches for tip motion:

- Manual segmentation + standard tracking ImageJ plug-in [6]. \rightarrow "Real" speed
- Automatic segmentation + OF with optimum parameters \rightarrow OF-estimated speed
- Automatic segmentation + standard tracking ImageJ plug-in. \rightarrow Tracking-estimated speed

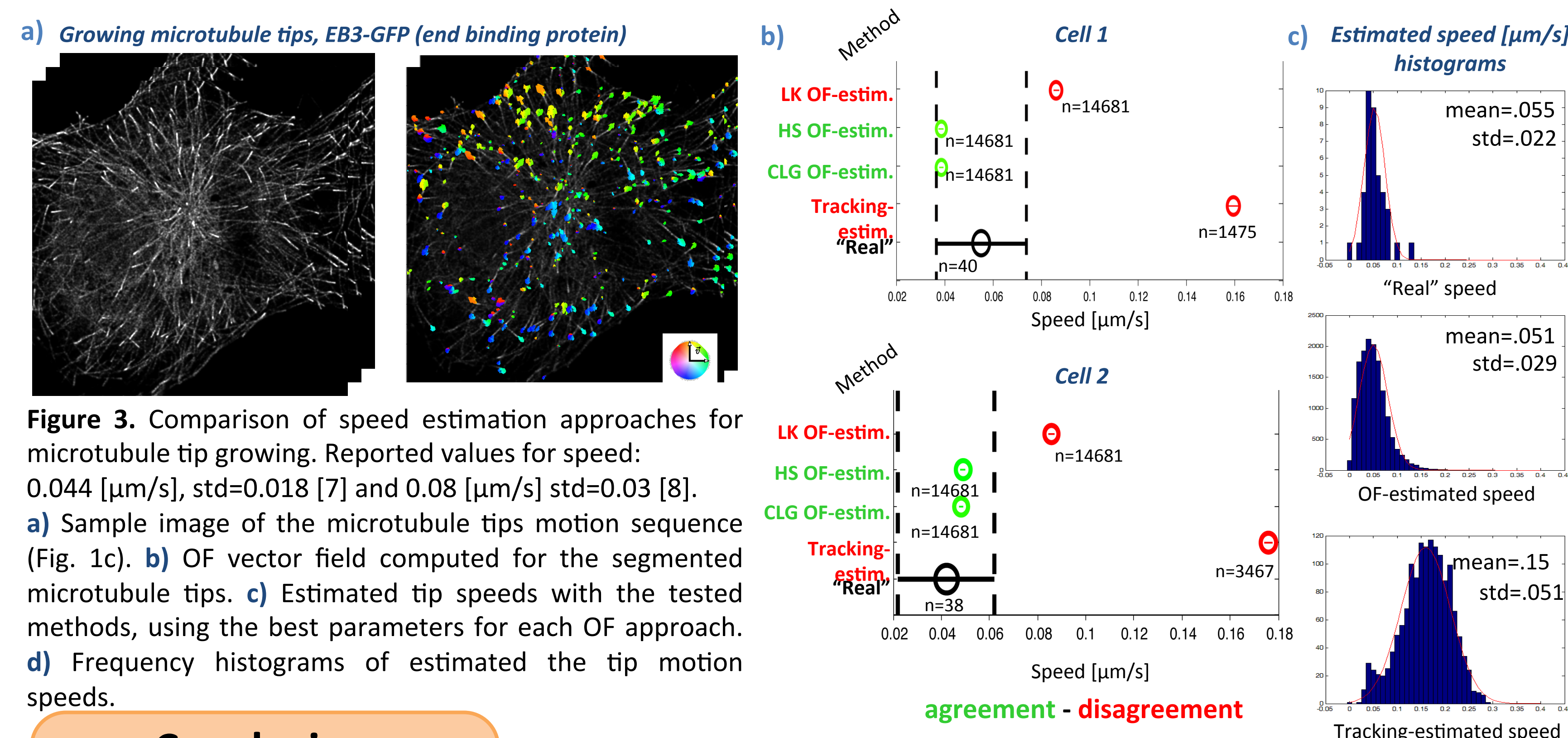


Figure 3. Comparison of speed estimation approaches for microtubule tip growing. Reported values for speed: 0.044 [μ m/s], std=0.018 [7] and 0.08 [μ m/s] std=0.03 [8].

- Sample image of the microtubule tips motion sequence (Fig. 1c).
- OF vector field computed for the segmented microtubule tips.
- Estimated tip speeds with the tested methods, using the best parameters for each OF approach.
- Frequency histograms of estimated the tip motion speeds.

Conclusion

MS-OF improves OF motion estimation range by a factor of three, and the performance of HS and CLG methods are comparable at least in the case of tip growing. We quantify and bound OF error for motion estimation in model structures. These results can be used directly to guide biologists in defining experimental spatio-temporal sampling acquisition rates and parameter settings when using OF for motion estimation and segmentation in time series.

When compared with automatic tracking, OF shows to be less sensitive to parameters, and its performance is comparable to manual segmentation and tracking performed by an expert.

References

- Horn BKP & Schunck BG (1981) Determining optical flow. Artificial Intelligence, Vol. 17: 185–203.
- Lucas BD (1985) Generalized image matching by the method of differences. PhD thesis, Robotics Institute, Carnegie Mellon University, Pittsburgh, PA, USA.
- Bruhn A & Weickert J (2005) Lucas/Kanade Meets Horn/Schunck: Combining Local and Global Optic Flow Methods. Int. J. of Computer Vision 61(3): 211-231.
- Delpiano J, Jara J, Scheer J, Ramírez O, Ruiz-del-Solar J and S Härtel (2012) Performance of optical flow techniques for motion analysis of fluorescent point signals in confocal microscopy. Machine Vision and Applications: 23(4):675-689.
- Márquez-Valle P, Gil D & Hernández-Sabaté A (2012) Error analysis for Lucas-Kanade Based Schemes. LNCS Vol. 7324: 184-191.
- Stuurman N (2003-9) ImageJ MTrack2 tracking plug-in. Ronald D. Vale Lab. at U. of California, San Francisco. <http://valelab.ucsf.edu/~nico/IJplugins/MTrack2.html>
- Friedman JR et al (2010) ER sliding dynamics and ER-mitochondrial contacts occur on acetylated microtubules. J. Cell Biol. Vol. 190 (3): 363–375.
- Cai D et al (2009) Single molecule imaging reveals differences in microtubule track selection between kinesin motors. PLoS Biology 7(10) e1000216.